



# Biaxial flexural strength and phase transformation of Ce-TZP/Al<sub>2</sub>O<sub>3</sub> and Y-TZP core materials after thermocycling and mechanical loading

Merve Bankoğlu Güngör<sup>1</sup>, Handan Yılmaz<sup>1\*</sup>, Cemal Aydın<sup>1</sup>, Seçil Karakoca Nemli<sup>1</sup>, Bilge Turhan Bal<sup>1</sup>, Tülay Tıraş<sup>2</sup>

<sup>1</sup>Department of Prosthodontics, Faculty of Dentistry, Gazi University, Ankara, Turkey

<sup>2</sup>Department of Physics, Faculty of Science, Anadolu University, Eskişehir, Turkey

**PURPOSE.** The purpose of the present study was to evaluate the effect of thermocycling and mechanical loading on the biaxial flexural strength and the phase transformation of one Ce-TZP/Al<sub>2</sub>O<sub>3</sub> and two Y-TZP core materials. **MATERIALS AND METHODS.** Thirty disc-shaped specimens were obtained from each material. The specimens were randomly divided into three groups (control, thermocycled, and mechanically loaded). Thermocycling was subjected in distilled water for 10000 cycles. Mechanical loading was subjected with 200 N loads at a frequency of 2 Hz for 100000 times. The mean biaxial flexural strength and phase transformation of the specimens were tested. The Weibull modulus, characteristic strength, 10%, 5% and 1% probabilities of failure were calculated using the biaxial flexural strength data. **RESULTS.** The characteristic strengths of Ce-TZP/Al<sub>2</sub>O<sub>3</sub> specimens were significantly higher in all groups compared with the other tested materials ( $P<.001$ ). Statistical results of X-ray diffraction showed that thermocycling and mechanical loading did not affect the monoclinic phase content of the materials. According to Raman spectroscopy results, at the same point and the same material, mechanical loading significantly affected the phase fraction of all materials ( $P<.05$ ). **CONCLUSION.** It was concluded that thermocycling and mechanical loading did not show negative effect on the mean biaxial strength of the tested materials. [J Adv Prosthodont 2014;6:224-32]

**KEY WORDS:** Ce-TZP/Al<sub>2</sub>O<sub>3</sub>; Y-TZP; Phase transformation; Thermocycling; Mechanical loading; Characteristic strength

Corresponding author:

Handan Yılmaz

Gazi University Faculty of Dentistry, Department of Prosthodontics,  
Emek 8.cad. 82.sok, 06510, Ankara, Turkey

Tel. 903122034196; e-mail, hozkula@gmail.com

Received December 19, 2013 / Last Revision April 30, 2014 / Accepted  
May 7, 2014

© 2014 The Korean Academy of Prosthodontics

This is an Open Access article distributed under the terms of the Creative Commons Attribution Non-Commercial License (<http://creativecommons.org/licenses/by-nc/3.0>) which permits unrestricted non-commercial use, distribution, and reproduction in any medium, provided the original work is properly cited.

This study was supported by the grant no. 03/2011-08 from Scientific Research Project of the Rectorship of Gazi University, Republic of Turkey. We thank to Panasonic Electric Works (Osaka, Japan) and 3M Espe (Seefeld, Germany) for kindly providing the materials used in this study. This work was presented at 19th Congress of the Balkan Stomatological Society, April 24-27, 2014, Belgrade, Serbia.

## INTRODUCTION

Y-TZP (yttria stabilized tetragonal zirconia polycrystals) are commonly used core materials that are manufactured from fine zirconia (ZrO<sub>2</sub>) particles and 1.75-3.5 mol.% yttrium oxide (Y<sub>2</sub>O<sub>3</sub>).<sup>1-3</sup> Y<sub>2</sub>O<sub>3</sub> is commonly used for stabilizing zirconia-based ceramics at room temperature.<sup>3,4</sup> However, cerium oxide can also be used to stabilize the tetragonal phase of zirconia.<sup>3,5</sup> Adding cerium oxide to the zirconia stabilizes its tetragonal phase under chemical and thermal conditions.<sup>6</sup> Because of the low strength of Ce-TZP (ceria stabilized tetragonal zirconia polycrystals), a combination of alumina-zirconia is decided to improve the strength of the material.<sup>6,7</sup>

Recently, a new type of zirconia ceramic, which is called

ceria-stabilized tetragonal zirconia/alumina (Ce-TZP/Al<sub>2</sub>O<sub>3</sub>) nanocomposite, has been developed.<sup>7-9</sup> Ce-TZP/Al<sub>2</sub>O<sub>3</sub> nanocomposite has an interpenetrated nanostructure and consists of 10 mol% Ce-TZP and 30 vol.% Al<sub>2</sub>O<sub>3</sub>.<sup>7,10,11</sup> The homogeneously dispersed Al<sub>2</sub>O<sub>3</sub> phase increases the hardness, elasticity modulus, and hydrothermal stability.<sup>12,13</sup>

Evaluating the characteristics under thermocycling and mechanical loading is crucial for the success of zirconia-based restorations because they are exposed to both thermal and mechanical fatigue in the oral environment.<sup>14</sup> Thermal and mechanical stresses may affect the materials' strength and clinical performance. On the other hand, phase transformations may be triggered by mechanical<sup>2</sup> and thermal fatigue,<sup>15</sup> and fatigue causes progression of subcritical cracks.<sup>2,16</sup>

The effect of different aging procedures on Ce-TZP/Al<sub>2</sub>O<sub>3</sub> has been studied in several investigations.<sup>11,15,17-20</sup> After storing in water and artificial saliva,<sup>15</sup> physiological saline solution,<sup>11,19</sup> acetic acid<sup>11,19</sup> and autoclave,<sup>11,15,17,19</sup> Ce-TZP/Al<sub>2</sub>O<sub>3</sub> showed satisfactory phase and mechanical durability versus to aging.<sup>11,19</sup> These experimental conditions do not fully reflect the oral environment. Restorative materials are exposed to saliva, acidification, thermal and mechanical cyclic stresses in the oral cavity. The reported comfortable temperature ranges between 15°C and 55°C.<sup>21</sup> Fontijn-Tekamp *et al.*<sup>22</sup> reported that physiological forces range from 60 to 75 N in the anterior dentition and from 110 to 125 N in the posterior dentition. However, maximum forces ranged from 140 to 170 N, and 250 to 400 N in anterior and posterior regions, respectively.<sup>22</sup> Investigating the mechanical properties of the newly developed materials under simulated oral cavity conditions and comparing the results with commonly used core materials are needed for defining their clinical acceptance. The purpose of this study was to evaluate the effect of thermocycling and mechanical loading on the biaxial flexural strength and the phase transformation of Ce-TZP/Al<sub>2</sub>O<sub>3</sub> and compare the results with two Y-TZP core materials.

## MATERIALS AND METHODS

Three groups were designed to investigate the effect of thermocycling and mechanical loading on zirconia-based core materials. Two yttria-stabilized zirconias; Cercon Base (Cercon, Degudent, Hanau, Germany) and Lava Plus (Lava, 3M ESPE, Seefeld, Germany) and one ceria-stabilized zirconia; NanoZR (Panasonic Electric Works, Osaka, Japan) were used in this study (Table 1). Manufacturers provided 30 disc-shaped specimens from each material. The specimens were 1.2 mm in thickness and 15 mm in diameter. The dimensions were selected according to ISO 6872<sup>23</sup> and were verified using an electronic digital micrometer (Powertechtools, Zhejiang, China).

Three experimental groups (n = 10) were created from each kind of material. Control specimens were in Group 1 and were abbreviated as CC for Cercon Base, LC for Lava Plus, and NC for NanoZR. Thermocycled specimens were in Group 2 and were abbreviated as CT, LT, and NT, for Cercon Base, Lava Plus, and NanoZR, respectively. Thermocycling was subjected in distilled water at 5 and 55°C for 10000 cycles in a thermocycling machine (Nüve, Ankara, Turkey). During a cycle, specimens were stored for 30 seconds in each bath.<sup>14,15,21</sup> The mechanical loading group was Group 3. For mechanical loading, the specimens were positioned on the supporting balls which were described in ISO 6872.<sup>23</sup> Specimens in Group 3 were abbreviated as CM, LM, and NM for Cercon Base, Lava Plus, and NanoZR, respectively. The mechanical loading was subjected with 200 N loads and a frequency of 2 Hz for 100000 times with a mechanical cyler (Instron 8801, Instron, Canton, MA) at the room conditions (22 ± 1°C, and 60 ± 5% relative humidity).<sup>2</sup>

The test was carried out after thermocycling and mechanical loading with a tension-compression test machine (Middle East Technical University, Department of Metallurgy, Ankara, Turkey). The speed of the machine was 0.15 mm/min. The specimens were tested with a technique

**Table 1.** Description of the tested materials

| Material    | Manufacturer                                   | Content                               | Composition  |
|-------------|--|---------------------------------------|--|
| Cercon Base | Cercon, Degudent, Hanau, Germany               | Y-TZP                                 | Zirconia<br>Yttrium oxide 5%<br>Hafnium oxide < 2%<br>Aluminium oxide and silicone oxide <1% |
| Lava Plus   | Lava, 3M ESPE, Seefeld, Germany                | Y-TZP                                 | Zirconia<br>Yttrium oxide 3%<br>Aluminium oxide 0.1 wt%                                      |
| NanoZR      | NanoZR, Panasonic Electric Works, Osaka, Japan | Ce-TZP/Al <sub>2</sub> O <sub>3</sub> | 10 mol % CeO <sub>2</sub> -ZrO <sub>2</sub><br>30 vol % Al <sub>2</sub> O <sub>3</sub>       |

of piston on three balls, which was identified in the standard of ISO 6872.<sup>23</sup> Three hardened steel balls (Turkish Aerospace Industries Inc., Ankara, Turkey), 3.2 mm in diameter, were placed at an angle of 120 degrees relative to each other to support the specimens. Each specimen was located on these supports of the testing machine and the centers of the specimens were loaded (Fig. 1). The load was applied with a flat punch (1.4 mm in diameter) until a fracture occurred. The biaxial flexural strengths of the specimens were calculated with the following formula:<sup>23</sup>

$$S = -0.2387 P (X - Y) / d^2,$$

where S is the flexural strength at fracture (MPa); P is the total load causing fracture (N),

$$X = (1 + \nu) \ln(r2 / r3)^2 + [(1 - \nu) / 2](r2 / r3)^2,$$

$$Y = (1 + \nu)[1 + \ln(r1 / r3)^2] + (1 - \nu)(r1 / r3)^2,$$

and  $\nu$  is Poisson's ratio (if the value for the ceramic being studied is not known, Poisson's ratio of 0.25 is used); r1 is the radius of the support circle, r2 is the radius of the loaded area (mm), r3 is the radius of the specimen (mm), and d is the specimen thickness at the origin of fracture (mm). For this study,  $\nu = 0.25$ , r1 = 5 mm, r2 = 0.7 mm, and r3 = 7.5 mm were used. The Weibull modulus, characteristic strength, 10%, 5% and 1% probabilities of failure were calculated using the biaxial flexural strength data.

Phase transformation was determined by XRD patterns of the control, thermocycling and mechanical loading specimens before the biaxial flexural strength test. The XRD patterns were recorded with an X-ray diffractometer (D/MAX 2200PC, Rigaku-Geirflex X-ray Diffractometer, Tokyo, Japan) by using Cu-K  $\alpha$ -radiation. Specimens were scanned at 40 kV, 40 mA, 0.018/step interval from 20-40,



**Fig. 1.** Placing test specimen on the supporting balls of the tension-compression machine.

and 20 degrees. The relative amount of the monoclinic phase ( $X_m$ ) was calculated with the following formula described by Garvie and Nicholson<sup>24</sup> for detecting the phase composition of zirconia:

$$X_m = (I_{m1} + I_{m2}) / (I_{m1} + I_{m2} + I_t),$$

where I is the intensity detected by the detector, t is the tetragonal peak, and m1 and m2 are the two major monoclinic peaks. The monoclinic phase content was determined by calculating the areas under the t, m1, and m2 peaks with MATLAB (MATLAB 2010 A, Mattworks, Natick, MA, USA).

Control, thermocycled, and mechanically loaded specimens were examined by a Raman spectrometer (Senterra; Bruker Optics GmbH, Ettlingen, Germany) before the strength test. The Raman laser was focused on center of the specimen (p1), the center of the radius of the specimen (p2), and the edge of the radius of the specimen (p3)(Fig. 2) at a wavelength of 520 nm and 20 mW power, 3  $cm^{-1}$  resolution, and 16 spectral integration times. The Raman intensity monoclinic ratio ( $X_m$ ) was calculated with the following formula:

$$X_m = I_m(180\text{ cm}^{-1}) + I_m(190\text{ cm}^{-1}) / I_m(180\text{ cm}^{-1}) + I_m(190\text{ cm}^{-1}) + I_t(147\text{ cm}^{-1})$$

where I corresponds the net peak intensities at the Raman shifts. By using the formula of Kim *et al.*,<sup>25</sup> the monoclinic fraction (fm) was calculated:

$$fm = (0.19 - 0.13 / (X_m - 1.01))^{1/2} - 0.56.$$

The flexural strength data were analyzed by using the two-parameter cumulative Weibull distribution, which is often used for ceramic materials because of their asymmetrical distribution. The Weibull moduli were calculated with the formula:<sup>23,26</sup>

$$P(\sigma) = 1 - \exp [-(\sigma / \sigma_0)^m],$$

where P is the fracture probability,  $\sigma$  is the fracture strength,  $\sigma_0$  is the characteristic strength at the fracture probability of 63.2%, and m is the Weibull modulus. In addition, the 10%, 5%, and 1% probabilities of failure were calculated. All results were evaluated according to the 0.001 significance level. The relative amount of monoclinic phase was analyzed by two-factor factorial ANOVA (analysis of

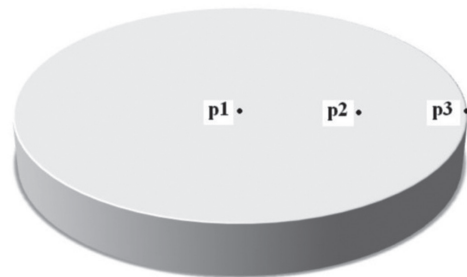


**Fig. 2.** Schematic diagram of three points (p1, p2, p3) where Raman spectra taken from.

variance). Significant differences with a significance level of  $\alpha=0.01$  (SPSS 18, SPSS Inc., Chicago, IL, USA) was determined with Duncan's multiple range test. The results of the monoclinic fraction were analyzed by three-factor ANOVA with repeated measures on each factor. Significant differences with a significance level of  $\alpha=0.05$  (SPSS 18, SPSS Inc., Chicago, IL, USA) were determined with Duncan's multiple range test.

## RESULTS

The Weibull statistical analyses, the characteristic strength, and the 10%, 5%, and 1% probabilities of failure are summarized in Table 2. The Weibull distributions of the tested groups are shown in Fig. 3, Fig. 4, and Fig. 5. The characteristic strengths of NanoZR were significantly higher in all materials ( $P<.001$ ), and the differences among the groups in NC, NT, and NM groups were not statistically significant

**Table 2.** Weibull statistical analysis

| Material/Experimental Group | Weibull Modulus $m$ (SE) | Characteristic strength (MPa) $\sigma_0$ (SE) | Strength for 10% probability of failure (MPa) $\sigma_{0.10}$ (SE) | Strength for 5% probability of failure (MPa) $\sigma_{0.05}$ (SE) | Strength for 1% probability of failure (MPa) $\sigma_{0.01}$ (SE) |
|-----------------------------|--------------------------|---|--|---|---|
| CC                          | 6.09 (1.52)              | 993.73 (54.55) <sup>a</sup>                   | 686.73   | 610.17  | 466.89  |
| CT                          | 7.24 (1.85)              | 977.68 (44.89) <sup>a</sup>                   | 716.48   | 648.67  | 517.91  |
| CM                          | 5.60 (1.39)              | 964.19 (57.37) <sup>a</sup>                   | 645.12   | 567.30  | 424.04  |
| LC                          | 12.36 (2.94)             | 1100.09 (29.76) <sup>a</sup>                  | 916.97   | 865.09  | 758.21  |
| LT                          | 9.42 (2.27)              | 1058.46 (37.66) <sup>a</sup>                  | 833.53   | 772.21  | 649.51  |
| LM                          | 14.99 (3.80)             | 1257.69 (27.75) <sup>b</sup>                  | 1082.36  | 1031.62   | 925.33  |
| NC                          | 21.82 (5.37)             | 1448.46 (22.21) <sup>c</sup>                  | 1306.52  | 1264.12   | 1173.13   |
| NT                          | 20.67 (4.67)             | 1497.43 (24.35) <sup>c</sup>                  | 1342.96  | 1297.00   | 1198.65   |
| NM                          | 21.25 (5.26)             | 1496.62 (23.53) <sup>c</sup>                  | 1346.23  | 1301.39   | 1205.30   |
| Chi-square                  | 39.383                   | 330.338                                       |  |   |   |
| <i>P</i> value              | <.001                    | <.001   |  |   |   |

Same small characters (vertically) indicate that  $\sigma_0$  values had no significant difference between groups ( $P>.001$ ).

Control, Thermocycled, mechanical loaded groups of Cercon, Lava, NanoZR were coded as CC, CT, CM, LC, LT, LM, NC, NT, and NM, respectively.

SE: Standard error of the mean.

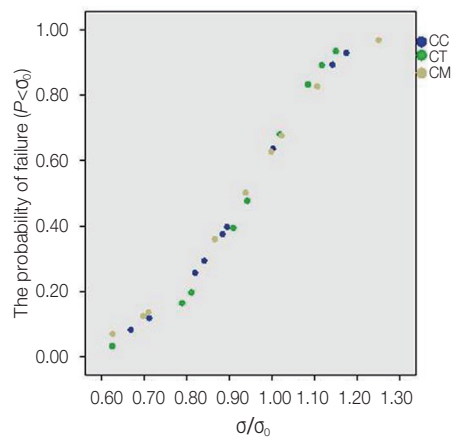


**Fig. 3.** Weibull moduli distribution of Cercon Base specimens.

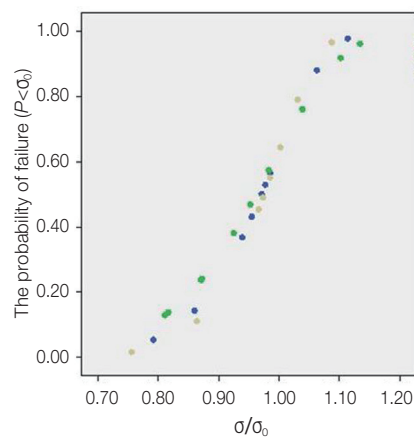


**Fig. 4.** Weibull moduli distribution of Lava Plus specimens.

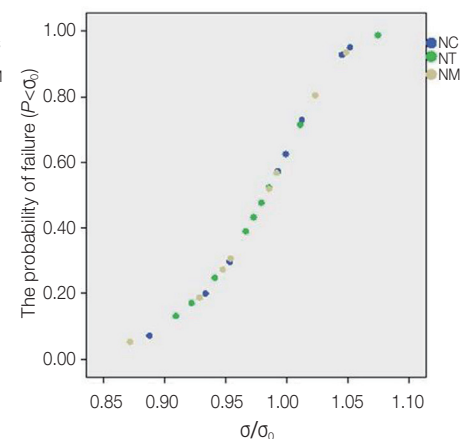


**Fig. 5.** Weibull moduli distribution of NanoZR specimens.

**Table 3.** Relative amount of monoclinic phase contents (%) of the experimental groups

| Experimental Groups (n = 10) | Cercon Base Mean (SE) | Lava Plus Mean (SE) | NanoZR Mean (SE) |
|------------------------------|-----------------------|---------------------|------------------|
| Control                      | 0.115 (0.02)          | 0                   | 5.917 (0.34)     |
| Thermocycling                | 0.197 (0.015)         | 0                   | 5.928 (0.22)     |
| Mechanical Loading           | 0.207 (0.026)         | 0.159 (0.02)        | 5.969 (0.39)     |

There were no statistical difference in control, thermocycling, and mechanical loading groups in same material.  
SE: Standard error of the mean.

( $P>.001$ ). The characteristic strength values of Lava Plus were higher than Cercon Base and lower than NanoZR. The characteristic strength values increased in the LM group, and it showed significant difference when compared with the LC and LT groups ( $P<.001$ ). Cercon Base had the lowest characteristic strength values in all the groups. However, the values were not statistically different within the Cercon Base groups ( $P>.001$ ). The Weibull moduli of NanoZR were higher when compared with the other materials. The Lava Plus values were higher than the Cercon Base values and lower than the NanoZR values. The values increased in the LM group in comparison with the LC and LM groups. The lowest values were observed in Cercon Base in all groups.

The monoclinic phase contents of the materials are shown in Table 3 and Table 4. The XRD patterns of one of the specimens in experimental groups are shown in Fig. 6, Fig. 7, and Fig. 8. Statistical results of XRD showed that thermocycling and mechanical loading did not affect the monoclinic phase content. The monoclinic phase contents were not statistically different between the control, thermocycled, and mechanically loaded specimens. However the

**Table 4.** Comparison of relative amount of monoclinic phases (%) of the materials

| Material    | N  | Mean (SE)                |
|-------------|----|--------------------------|
| Cercon Base | 30 | 0.17 (0.01) <sup>B</sup> |
| Lava Plus   | 30 | 0.05 (0.01) <sup>C</sup> |
| NanoZR      | 30 | 5.94 (0.18) <sup>A</sup> |

Same capital characters (vertically) indicate that relative amount of monoclinic phases had no significant difference within a group ( $P>.01$ ).  
SE: Standard error of the mean.

monoclinic phase content of the Cercon Base, Lava Plus and NanoZR specimens were statistically different ( $P<.01$ ). Monoclinic zirconia phases (JCPDS No. 37-1484) were detected in all groups except the control and thermal-aged specimens of Lava Plus. LC and LT groups were composed of 100% tetragonal zirconia (JCPDS No. 50-1089). The highest monoclinic phase content was observed in NanoZR and it was significantly different from other materials

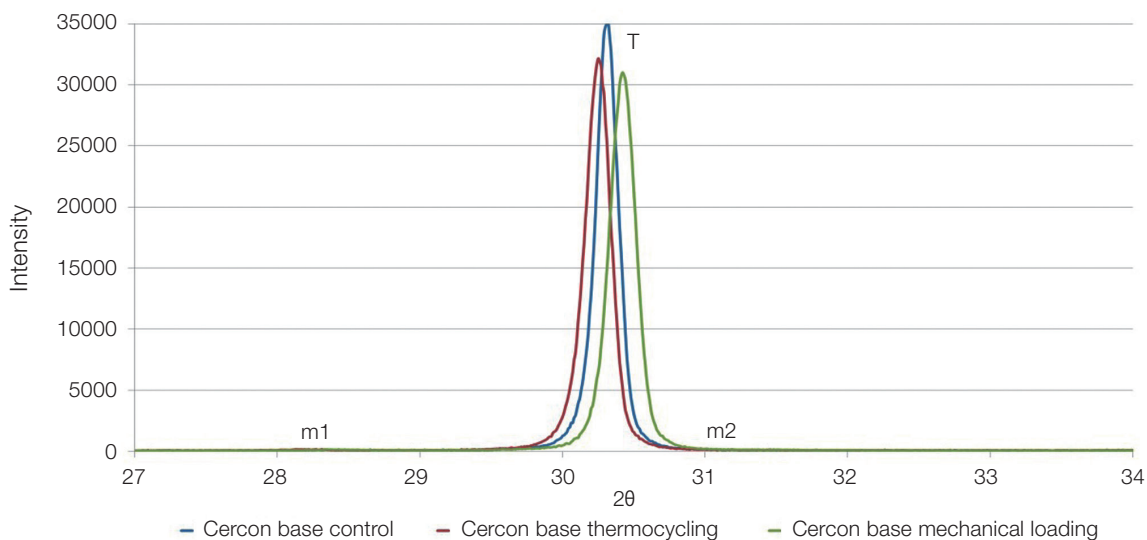


**Fig. 6.** XRD patterns of one of Cercon Base specimen from all experimental groups.

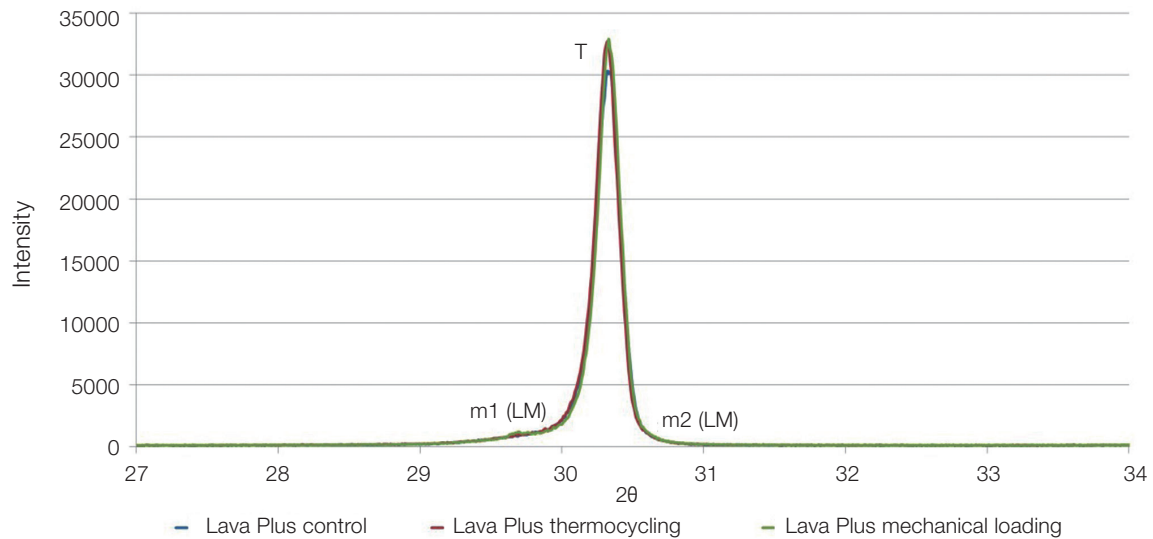


**Fig. 7.** XRD patterns of one of Lava Plus specimen from all experimental groups.

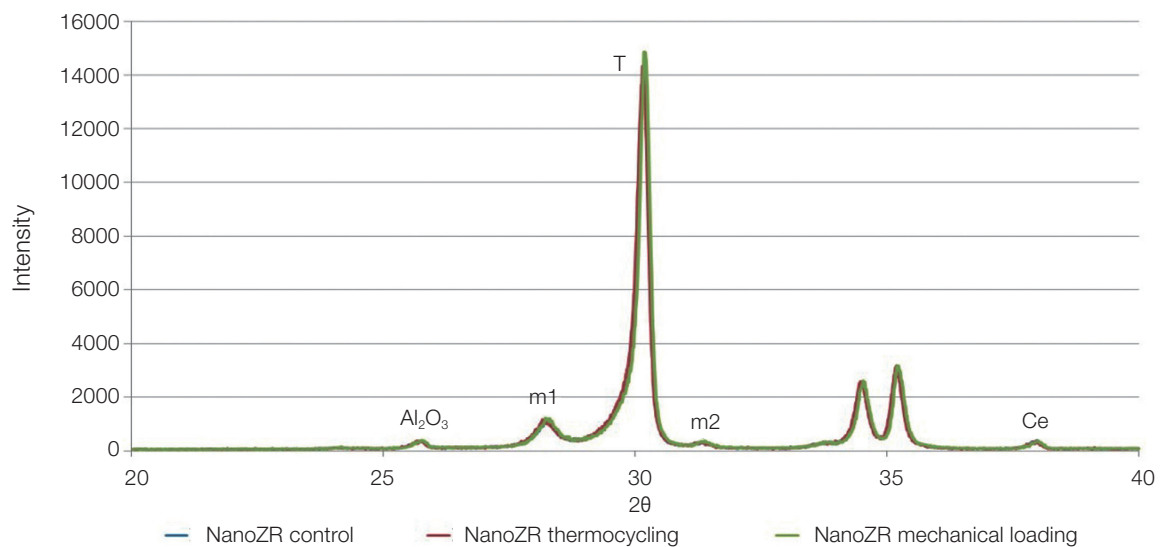


**Fig. 8.** XRD patterns of one of NanoZR specimen from all experimental groups.

( $P < .01$ ). The other constituents of NanoZR were; tetragonal zirconia (JCPDS No. 17-0923), monoclinic zirconia (JCPDS No. 37-1484), cerium (JCPDS No. 38-0762), and corundum (Al<sub>2</sub>O<sub>3</sub>) (JCPDS No. 10-0173). The lowest monoclinic phase content was observed in Lava Plus within the materials.

The monoclinic phase fraction of the Raman spectroscopy results are shown in Table 5. The Raman spectroscopy results showed that material type (C, L, and N), the point Raman spectra taken from (p1, p2, and p3), and the thermocycling and mechanical loading methods (C, T, and M) affected the monoclinic phase fraction. When comparing

the phase fraction of materials at the same point and the same method, except NM at point p1 and all groups in NanoZR at points p2 and p3, the differences were not significant in all materials ( $P > .05$ ). When comparing the points Raman spectra taken from the same material and the same method, except for NC and NT groups at point p2, the NM group at point p3, and LM group at points p1 and p2, the differences were not significant in all materials ( $P > .05$ ). When comparing the experimental groups at the same point and the same material, the mechanical loading groups showed significant differences in all materials ( $P < .05$ ).

**Table 5.** The mean values of monoclinic phase fractions (%) at each point

| Point          | Material/Experimental Group (n = 10) | Mean value (SE)                |
|----------------|--------------------------------------|--------------------------------|
| p1<br>(Center) | CC                                   | 0.434 (0.0005) <sup>Aax</sup>  |
|                | LC                                   | 0.438 (0.0012) <sup>Aax</sup>  |
|                | NC                                   | 0.434 (0.0014) <sup>Aax</sup>  |
|                | CT                                   | 0.435 (0.0007) <sup>Aax</sup>  |
|                | LT                                   | 0.436 (0.0011) <sup>Aax</sup>  |
|                | NT                                   | 0.432 (0.0015) <sup>Aax</sup>  |
|                | CM                                   | 0.429 (0.0006) <sup>Aay</sup>  |
|                | LM                                   | 0.426 (0.0004) <sup>Aby</sup>  |
|                | NM                                   | 0.419 (0.0009) <sup>Bay</sup>  |
| p2<br>(Middle) | CC                                   | 0.435 (0.0005) <sup>Aax</sup>  |
|                | LC                                   | 0.437 (0.0013) <sup>Aax</sup>  |
|                | NC                                   | 0.428 (0.0015) <sup>Bbx</sup>  |
|                | CT                                   | 0.435 (0.0005) <sup>Aax</sup>  |
|                | LT                                   | 0.436 (0.0010) <sup>Aax</sup>  |
|                | NT                                   | 0.429 (0.0010) <sup>Bbx</sup>  |
|                | CM                                   | 0.429 (0.0005) <sup>Aay</sup>  |
|                | LM                                   | 0.426 (0.0005) <sup>Aby</sup>  |
|                | NM                                   | 0.420 (0.0009) <sup>Bay</sup>  |
| p3<br>(Edge)   | CC                                   | 0.437 (0.0006) <sup>Aax</sup>  |
|                | LC                                   | 0.438 (0.0008) <sup>Aax</sup>  |
|                | NC                                   | 0.431 (0.0024) <sup>Bax</sup>  |
|                | CT                                   | 0.436 (0.0005) <sup>Aax</sup>  |
|                | LT                                   | 0.436 (0.0011) <sup>Aax</sup>  |
|                | NT                                   | 0.431 (0.0014) <sup>Babx</sup> |
|                | CM                                   | 0.430 (0.0005) <sup>Aay</sup>  |
|                | LM                                   | 0.430 (0.0007) <sup>Aay</sup>  |
|                | NM                                   | 0.419 (0.0010) <sup>Bby</sup>  |

Same capital alphabets (vertically) in same experimental method and same point indicate that material types had no significant difference between each other ( $P > .05$ ).

Same small alphabets (vertically) in same material and same experimental method indicate that points had no significant difference between each other ( $P > .05$ ).

Same small x and y alphabets (vertically) in same point and same material indicate that experimental methods had no significant difference between each other ( $P > .05$ ).

SE: Standard error of the mean.

## DISCUSSION

Zirconia-based restorations are exposed to temperature changes and cyclic stresses in the oral cavity.<sup>14</sup> Fatigue of these materials can cause detrimental effects on the mechanical properties of the materials.<sup>27</sup> Therefore, fatigue tests are essential to define mechanical properties and ensure the clinical success of these materials.<sup>27</sup> Some stud-

ies have stated that fatigue affects the mechanical properties of the zirconia-based core materials.<sup>2,11,14</sup>

Within the limitation of the present study, there were no significant differences in the strength of the core materials after thermocycling and mechanical loading. NanoZR had significantly higher characteristic strength values than the two other Y-TZP ceramics and there were no significant differences in the characteristic strength of NC, NT, and NM groups. NanoZR showed a high Weibull modulus (m) and demonstrated a low variability ranging from 20.67 to 21.82. A high Weibull modulus defines better clinical reliability of the materials.<sup>26,28</sup> The characteristic strength of LM group was significantly higher than that of the LC and LT groups ( $P < .001$ ). The authors observed a similar increase in the strength of bilayered Lava specimens when subjected to 20000 mechanical loadings in a previous study.<sup>2</sup> The observed m values for Lava Plus were 12.36 for the control group and 14.99 for the mechanical loading group. The characteristic strengths of Cercon Base were not significantly different in all groups ( $P > .001$ ); the m values of the Cercon Base were between 5.6 and 7.24. In the present study, NanoZR had the highest characteristic strengths. This finding may be result of NanoZR's interpenetrated intragranular nanostructure and composition. Nano-meter-sized Ce-TZP/ $Al_2O_3$ , which has strong mechanical properties and stability against aging, has been developed by Nawa *et al.*<sup>10</sup> and its properties have been demonstrated in some studies.<sup>9,11,15</sup> Ban *et al.*<sup>11</sup> found that nanostructured Ce-TZP/ $Al_2O_3$  had durability against aging and there were no significant phase transformation under different storage conditions.

Stress-induced phase transformation is an important factor for strengthening TZP.<sup>29</sup> In the present study, the biaxial flexural strengths of NanoZR groups were not statistically significant from each other and the values in the LM group were significantly higher than in the LT and LC groups ( $P < .001$ ). Borchers *et al.*<sup>14</sup> researched the influence of different environmental and loading conditions on the biaxial strength of two different 3Y-TZP. It was concluded that Y-TZP ceramics showed phase transformations after different hydrothermal treatments. However, their strengths were not significantly influenced because the transformation depths did not progress enough from the surfaces into the materials.<sup>14</sup> Cattani-Lorente *et al.*<sup>1</sup> demonstrated similar results and stated that the transformation occurred in a 6  $\mu$ m thick subsurface layer. In the present study, the specimens were subjected to 10000 thermocycles or 100000 mechanical cycles. The specimens were not affected negatively by the cycling conditions; this result was consistent with the fact that the transformation was not deep enough to extend into the material under these thermal and mechanical cycles. In the present study, results of both thermocycling and mechanical loading methods did not significantly affect the phase transformation of the materials. Yilmaz *et al.*<sup>2</sup> reported that the monoclinic phase content of the Lava and Cercon specimens significantly increased after 20000 mechanical cycles. The CC and LC groups consisted

of tetragonal zirconia but the monoclinic contents of the specimens increased after mechanical loading. In the present study, the difference in the monoclinic phase contents of the materials was not statistically significant after thermocycling and mechanical loading. The monoclinic content was not detected in the LC and LT groups. However, the monoclinic phase content of the LM group was significantly higher than that of the LC and LT groups. The difference in the amount of monoclinic phase between the two Y-TZP core ceramics may be a result of the difference in the intrinsic structure or sintering schedule.<sup>15</sup> The amount of the monoclinic phase of NanoZR ranged from  $5.917 \pm 0.34\%$  to  $5.969 \pm 0.39\%$ . A similar monoclinic content, ranging from 4.8 to 5.5%, was reported by Ban *et al.*<sup>11</sup> Perdigão *et al.*<sup>15</sup> evaluated the effect of hydrothermal fatigue on ZrO<sub>2</sub>-based (Lava, IPS and NanoZR) materials. The specimens were stored in water, autoclaved or thermocycled in artificial saliva for 30000 thermal cycles. The observed values in the present study were lower than the values presented by Perdigão *et al.*<sup>15</sup> Although both studies used the same thermocycling conditions, the difference may originate from the higher number of cycles used in the study of Perdigão *et al.*<sup>15</sup>

The monoclinic phase contents of the zirconia-based materials can be detected with Raman spectroscopy. Raman spectroscopy is able to detect very small regions on a specimen surface without preparation<sup>30</sup> and can be useful for defining the amount of monoclinic phase.<sup>25</sup> Sato *et al.*<sup>18</sup> evaluated the mechanical properties of Ce-TZP/Al<sub>2</sub>O<sub>3</sub> and Y-TZP after sandblasting and heat treatment and detected the phase changes with Raman spectroscopy. Raman analyses showed that the transformation zone depth was approximately less than 10 μm and that the biaxial flexural strength increased after sandblasting but decreased after heat treatment.<sup>18</sup> In the present study, the transformation zone depths were not detected by Raman spectroscopy but the Raman spectra were taken from three different points on the surface of the specimens. In the present study, according to XRD results, the monoclinic phase contents of the materials were not affected by the experiments. However, it was detected that the phase fraction of the materials was significantly affected by thermocycling and mechanical loading when the Raman spectra were obtained from different points on the surface of the specimens ( $P < .05$ ). Furthermore, it was observed that the results were significantly lower in mechanical loading groups at the same point and the same material ( $P < .05$ ). During mechanical loading, the core materials are subjected to highly localized stresses. Behrens *et al.*<sup>31</sup> stated that applied loads triggered phase transformation and that compressive stresses were higher in the indentation center. The monoclinic phase fractions were found lower at the center of the indent when compared to edge of the indent.<sup>31,32</sup> In the present study, specimens were subjected to 100000 mechanical cycles under 200 N and the lower monoclinic phase fraction may be a result of the concentrated compressive stresses on the specimens during mechanical loading.

Y-TZP is a frequently used core material in fixed partial prosthesis. Ce-TZP/Al<sub>2</sub>O<sub>3</sub> is a novel material with a high mechanical strength and resistance to fatigue. The results of the study showed that both materials have reliability and can be used clinically. However, further experiments related to the effect of the firing processes, surface treatments on the porcelain connection values of bilayered specimens, and clinical applications are needed to evaluate the long-term behavior of this new material.

## CONCLUSION

Within the limitations of this study, the X-ray diffraction results showed that thermocycling and mechanical loading did not have a significant effect on the phase transformation of the tested materials. However, Raman spectroscopy results showed that monoclinic phase fraction of the mechanically loaded specimens were lower at the point p1 where the load was applied. Furthermore, it was concluded that the characteristic strengths of all the tested materials were not affected negatively by thermocycling and mechanical loading and all the tested materials have reliability in clinical use.

## REFERENCES

1. Cattani-Lorente M, Scherrer SS, Ammann P, Jobin M, Wiskott HW. Low temperature degradation of a Y-TZP dental ceramic. *Acta Biomater* 2011;7:858-65.
2. Yilmaz H, Nemli SK, Aydin C, Bal BT, Tıraş T. Effect of fatigue on biaxial flexural strength of bilayered porcelain/zirconia (Y-TZP) dental ceramics. *Dent Mater* 2011;27:786-95.
3. Piconi C, Maccauro G. Zirconia as a ceramic biomaterial. *Biomaterials* 1999;20:1-25.
4. Kohorst P, Borchers L, Stempel J, Stiesch M, Hassel T, Bach FW, Hübsch C. Low-temperature degradation of different zirconia ceramics for dental applications. *Acta Biomater* 2012;8:1213-20.
5. Yang G, Li JC, Wang GC, Yashima M, Min SL, Chen TC. Investigation on strengthening and toughening mechanisms of Ce-TZP/Al<sub>2</sub>O<sub>3</sub> nanocomposites. *J Metall Mater Trans A* 2006;37:1969-75.
6. Mangalaraja RV, Chandrasekhar BK, Manohar P. Effect of ceria on the physical, mechanical and thermal properties of yttria stabilized zirconia toughened alumina. *Mater Sci Eng A* 2003;343:71-5.
7. Nawa M, Nakamoto S, Sekino T, Niihara K. Tough and strong Ce-TZP/Alumina nanocomposites doped with titania. *Ceram Int* 1998;24:497-506.
8. Ban S. Reliability and properties of core materials for all-ceramic dental restorations. *Jpn Dent Sci Rev* 2008;44:3-21.
9. Tanaka K, Tamura J, Kawanabe K, Nawa M, Uchida M, Kokubo T, Nakamura T. Phase stability after aging and its influence on pin-on-disk wear properties of Ce-TZP/Al<sub>2</sub>O<sub>3</sub> nanocomposite and conventional Y-TZP. *J Biomed Mater Res A* 2003;67:200-7.
10. Nawa M, Bamba N, Sekino T, Niihara K. The effect of TiO<sub>2</sub>



- addition on strengthening and toughening in intragranular type of 12Ce-TZP/ $\text{Al}_2\text{O}_3$  nanocomposites. *J Eur Ceram Soc* 1998;18:209-19.
11. Ban S, Sato H, Suehiro Y, Nakanishi H, Nawa M. Biaxial flexure strength and low temperature degradation of Ce-TZP/ $\text{Al}_2\text{O}_3$  nanocomposite and Y-TZP as dental restoratives. *J Biomed Mater Res B Appl Biomater* 2008;87:492-8.
  12. Hirano M, Inada H. Fracture toughness, strength and Vickers hardness of yttria-ceria-doped tetragonal zirconia/alumina composites fabricated by hot isostatic pressing. *J Mater Sci* 1992;27:3511-8.
  13. Fischer J, Stawarczyk B. Compatibility of machined Ce-TZP/ $\text{Al}_2\text{O}_3$  nanocomposite and a veneering ceramic. *Dent Mater* 2007;23:1500-5.
  14. Borchers L, Stiesch M, Bach FW, Buhl JC, Hübsch C, Kellner T, Kohorst P, Jendras M. Influence of hydrothermal and mechanical conditions on the strength of zirconia. *Acta Biomater* 2010;6:4547-52.
  15. Perdígão J, Pinto AM, Monteiro RC, Braz Fernandes FM, Laranjeira P, Veiga JP. Degradation of dental  $\text{ZrO}_2$ -based materials after hydrothermal fatigue. Part I: XRD, XRF, and FESEM analyses. *Dent Mater J* 2012;31:256-65.
  16. Pittayachawan P, McDonald A, Petrie A, Knowles JC. The biaxial flexural strength and fatigue property of Lava Y-TZP dental ceramic. *Dent Mater* 2007;23:1018-29.
  17. Ban S, Suehiro Y, Nakanishi H, Nawa M. Fracture toughness of dental zirconia before and after autoclaving. *J Ceram Soc Jpn* 2010;118:406-9.
  18. Sato H, Yamada K, Pezzotti G, Nawa M, Ban S. Mechanical properties of dental zirconia ceramics changed with sandblasting and heat treatment. *Dent Mater J* 2008;27:408-14.
  19. Nakamura T, Yamashita K, Neo M. Mechanical properties of zirconia/alumina nano-composite after soaking in various water-based conditions. *Key Eng Mater* 2006;309-11:1219-22.
  20. Takano T, Tasaka A, Yoshinari M, Sakurai K. Fatigue strength of Ce-TZP/ $\text{Al}_2\text{O}_3$  nanocomposite with different surfaces. *J Dent Res* 2012;91:800-4.
  21. Gale MS, Darvell BW. Thermal cycling procedures for laboratory testing of dental restorations. *J Dent* 1999;27:89-99.
  22. Fontijn-Tekamp FA, Slagter AP, Van Der Bilt A, Van 't Hof MA, Witter DJ, Kalk W, Jansen JA. Biting and chewing in overdentures, full dentures, and natural dentitions. *J Dent Res* 2000;79:1519-24.
  23. ISO 6872. Dentistry-ceramic materials. Geneva; Switzerland; International Organization for Standardization; 2008.
  24. Garvie RC, Nicholson PS. Phase analysis in zirconia systems. *J Am Ceram Soc* 1972;55:303-5.
  25. Kim BK, Hahn JW, Han KR. Quantitative phase analysis in tetragonal-rich tetragonal/monoclinic two phase zirconia by Raman spectroscopy. *J Mater Sci Lett* 1997;16:669-71.
  26. Bona AD, Anusavice KJ, DeHoff PH. Weibull analysis and flexural strength of hot-pressed core and veneered ceramic structures. *Dent Mater* 2003;19:662-9.
  27. Studart AR, Filser F, Kocher P, Gauckler LJ. Fatigue of zirconia under cyclic loading in water and its implications for the design of dental bridges. *Dent Mater* 2007;23:106-14.
  28. Karakoca S, Yilmaz H. Influence of surface treatments on surface roughness, phase transformation, and biaxial flexural strength of Y-TZP ceramics. *J Biomed Mater Res B Appl Biomater* 2009;91:930-7.
  29. Gupta TK, Lange FF, Bechtold JH. Effect of stress-induced phase transformation on the properties of polycrystalline zirconia containing metastable tetragonal phase. *J Mater Sci* 1978;13:1464-70.
  30. Kailer A, Nickel KG, Gogotsi YG. Raman microspectroscopy of nanocrystalline and amorphous phases in hardness indentations. *J Raman Spectrosc* 1999;30:939-46.
  31. Behrens G, Dransmann GW, Heuer AH. On the isothermal martensitic transformation in 3Y-TZP. *J Am Ceram Soc* 1993;76:1025-30.
  32. Nemli SK, Yilmaz H, Aydın C, Bal BT, Tıraş T. Effect of fatigue on fracture toughness and phase transformation of Y-TZP ceramics by X-ray diffraction and Raman spectroscopy. *J Biomed Mater Res B Appl Biomater* 2011 Nov 21.